CONEM 2016
CONGRESSO NACIONAL DE ENGENHARIA MECÂNICA
21 - 25 AGOSTO DE 2016
FORTALEZA - CEARÁ
ABCM 40 anos
Associação Brasileira de Engenharia e Ciências Mecânicas

POST-PROCESSING OF X-RAY TOMOGRAPHIC IMAGES OF AN ACOUSTIC FIBROUS MATERIAL AND POSSIBLE USE OF NUMERICAL METHODS SUCH AS FEM AND LBM TO DETERMINE BIOT'S POROUS TECHNICAL PARAMETERS.

Belisario Nina Huallpa, e-mail: belisario.nina@deg.ufla.br[1]
José Roberto de F. Arruda, e-mail: arruda@fem.unicamp.br[2]
Francisco Ilson da Silva Júnior, e-mail: ilson@ufc.br[3]
Pierre Lamary, e-mail: pierre.lamary@ufc.br[3]

[1]Engineering Department, Federal University of Lavras (UFLA), Caixa Postal 3037, CEP 37200-000, Lavras, MG, Brazil
[2]Department of Computational Mechanics, Faculty of Mechanical Engineering, State University of Campinas (Unicamp), Cidade Universitária "Zeferino Vaz- Barão Geraldo - Caixa Postal 6122 - CEP: 13083-970, Campinas, SP, Brazil
[3]Department of Mechanical Engineering, Federal University of Ceará (UFC), Campus do Pici - Bloco 714 - CEP 60455-760, Fortaleza, CE, Brazil

Abstract: *This work is part of a project centred on the mechanical and acoustical characterisation of materials supported by coconut fibres from which acoustic absorbing materials made of coconut fibres saturated by air. The material is highly porous and the characterization aims at determining the parameters of the homogenized equilibrium equations of Biot and of the semi-phenomenological micro-macro model of Johnson-Champoux-Allard (JCA). Two approaches have been followed. The first is an indirect method, which is based on the use of impedance tubes and then applying an inverse characterization technique. The second is a direct method based on the analysis of tomographic images of material samples. The two approaches are complementary because any parameter which can be directly determined will ease the indirect parameters estimation. In particular, among the five parameters we are looking for (Porosity, Tortuosity, Air flow resistance, Viscous characteristic length, and Thermal characteristic length), two play a special role, the porosity and the resistivity . When both porosity and air flow resistance are known, there exist many inverse estimation methods (that are straightforward to implement experimentally, for instance using impedance tubes) which lead to the determination of the other parameters. This paper focuses on the direct approach based on the post-processing of tomographic images to determine theses two fundamental parameters. The difficulty is that the tomography produces, slice by slice, two dimensional images that are given in a grey color scale. The post-processing consists in the analysis of the grey images in order to identify the geometry and the location of the fibres, so as to be able to produce black and white images for this bi- phase material. From this, the porosity of the sample is deduced counting the black and white pixels. Several image processing algorithms are compared in this work for our coconut fibre sample. The porosity varies from 0.76 to 0,97 depending of the methods and is finally estimated to be 0.86 from our analysis. For the Resistivity, the governing idea is to perform micro-scale numerical simulations. The software associated to the tomograph is able to produce 3D Finite Element meshes of the sample. However, we have encountered some limitations and have estimated that the FEM was not the proper method to be used as it is. Development based of quad-tri meshes and voxels meshes are planed. Therefore, we turn our attention to an another method, the LBM (Lattice Botlzmann Method) where the lattice is directly the pixels grid and which is able to solve Navier-Stokes equation. For the simulation, a constant fluid flow goes through the sample and a pressure drop is set from the input and output inlets. The internal velocity is computed and the Permeability (which is directly link to the Resistivity) is deduced. Using a black and white slice, obtained by the previous methods, 2D simulations were carried out and results were found to be very satisfactory in terms of methods performance. The iterative calculation lasts 1 minute on a common laptop and used only 200 Mo of memory. This indicates that 3D calculations will be accessible. The physical relevance of the value obtained was not addressed in this study and should to be part of coming works. To do this, 3D calculation will be needed because in the 2D situation the fluid cannot go around the fibres in the omitted direction. It will be also needed to imagine a reconstruction algorithm to get a black and white voxels 3D images with the appropriated porosity.*
Keywords: *LBM, acoustics, characterisation, porous, Biot, tomography.*

1. INTRODUCTION

Acoustic materials usually consist of a solid phase and a fluid phase. The waves propagating in the fluid can be attenuated when passing through the pores of the solid phase due to viscous and thermal dissipation mechanisms. This acoustic energy attenuation can be modelled using Biot's theory. Allard and Attala (2009) have applied Biot's theory to acoustic materials and their model, called Biot-Allard's model, is one of the most complex ones, taking into account viscous and thermal effects as well as the effect of the solid frame flexibility. In the limit cases where the solid frame is considered rigid or its stiffness is considered negligible (limp models), an equivalent fluid model can be used. One of the most complete models is the Johnson-Champoux-Allard model (JCA). In this model the acoustic material is characterized by five parameters: porosity, tortuosity, air flow resistance, viscous characteristic length, and thermal characteristic length. When both porosity and air flow resistance are known, there exist many parameter estimation methods that are straightforward to implement experimentally, for instance using impedance tubes, Pegoretti *et al.* (2014), Coser *et al.* (2014) and Coser *et al.* (2015).

Porosity is defined as the ratio of the volume occupied by the gas (usually air) to the total volume, Allard and Attala (2009). The total volume is the sum of the volume occupied by the gas and the volume occupied by the solid frame. Porosity must be measured or computed for a representative volume of the acoustic material. A representative volume has a characteristic length much smaller than the wavelength of the waves in the audio frequency domain and much larger than the random microscopic features of the material, so that average properties of the homogenized material can be obtained.

Traditional methods used to experimentally estimate porosity can be classified in two types. Direct methods consist of the immersion of a sample of the porous material in a fluid (typically water) and computing the ratio of the volume of the fluid to the total volume of the sample, AFPC-AFREM (1997). Otherwise, if the mass density of the solid phase is known and homogeneous, from the weight of the sample, the volume of the solid frame can be computed and subtracted from the total volume obtained from the geometry of the sample. More precise methods are based upon gas expansion in cavities with known volume and pressure measurements, such as in the Boyle's Law Porosimeter (Salissou and Panneton, 2007).

In this work the use of an X-ray Computer Tomography (CT) to estimate the porosity of a fibrous acoustic material is investigated. The fibers are natural fibers obtained from the outer skin of coconuts. The fibers are sprayed with latex and compressed to form fibrous materials, Pennafort (2014). From this, we investigate the possible use of the FEM and the LBM to carried out numerical simulation in order to estimate the static air flow resistivity. To state the problem, the figure 1shows the 3D reconstruction of the image of one of our sample.

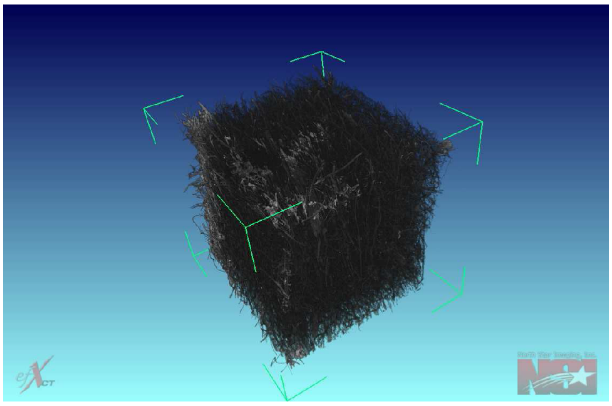

Figure 1: Tomographic 3D image reconstruction of the porous sample under study.

2. ESTIMATING POROSITY FROM XRCT IMAGES

The X-ray CT yields images that are slices of a sample, Keller (1998). The X-ray attenuation depends on the density of the material through which the radiation is transmitted. Using appropriate image processing transformations, it is possible to create an image of slices of a material sample. In the case of high energy X-rays (above 100 kV), Taud *et al.* (2005), these images the so-called CT number is correlated to mass density. Therefore, in principle it is possible to estimate the porosity of a sample of porous material using CT images. If an acoustic material is composed of a solid phase and a fluid phase (air in our case) it is likely that the solid phase has a higher density. Therefore, separating the solid from the fluid phase on the obtained images one can determine the volume of air as a percentage of the total volume i.e., the porosity. Usual CT images are calibrated so that water gives a value of zero for the CT value and air gives -1000. The solid phase has values typically larger than zero.

The major problem for estimating porosity from CT images is the segmentation process (thresholding) in order to separate air from solid. Visual thresholding is prone to subjective errors and lacks repeatability. A recent work by Taud *et al.* (2005) proposes a method based upon CT images to estimate porosity. Given a set of images representing the scan of a representative volume of the porous material, to each pixel (or voxel in the 3D case) of the image, a CT number ranging from 0 to r_{max} is attributed. They are typically gray scale image integer values. The range of CT values is divided into bins, and a histogram is computed, so that to each range of values r_i , $(i-1)\Delta r < r_i < i\Delta r$, has a count of n_i in a total number of pixels (or voxels) of n, with $H(r_i) = n_i/n$ and $\sum_{r_i=0}^{r_i=r_{max}} H(r_i) = 1$. In this case the porosity can be estimated with:

$$\Phi(r_{max}) = \frac{\sum_{r_i=0}^{r_i=r_{max}} (r_{max} - r_i)H(r_i)}{\sum_{r_i=0}^{r_i=r_{max}} r_{max}H(r_i)} \quad (1)$$

This value is computed for different values of r_{max} and the minimum of the obtained curve corresponds to the desired porosity. Depending on how the image is processed, the value of $1-\Phi$ can be obtained, as it is the case in the example treated in this work. The results obtained with this method are compared with the classical methods based on the thresholding approach, such as IsoData (Ridler and Calvard, 1978), Huang (Huang and Wang, 1995), Li (Li and Lee, 1993), Mean (Glasbey, 1993), Moments (Tsai, 1985), Otsu (Otsu, 1979), and Shanbhag (Shanbhag, 1994, September). These thresholding methods are available in the public open domain ImageJ (www.imagej.net) used in this work.

3. CT IMAGE-BASED POROSITY ESTIMATION RESULTS

A coconut fiber sample measuring approximately 50 x 50 x 50 mm was placed in the X-ray CT and 1158 slices were measured. It was observed that the slices with low noise were slices numbered between 150 and 939, which means 790 slices. After selecting the slices and applying a crop process, a 3D cube with dimensions of 40 x 40 x 40 mm with voxel size of 46.1 x 46.1 x 46.1 μm was selected. Figure 2 and 3 show respectively the coconut fiber specimen of initial size 50x50x45 mm3 and the X-ray CT of the cropped 3D image of the coconut fiber material sample of final size 40x40x40 mm3.

Figure 2: Coconut fiber specimen measuring 50x50x45 mm3

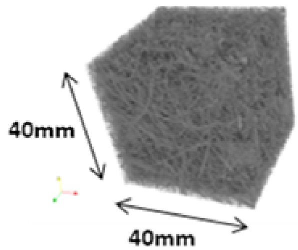

Figure 3: XRCT 3D cropped image.

The dimension of a slice of this 3D image is therefore 40 x 40 mm with a pixel size of 46.1 x 46.1 μm. The thickness is 46,1 μm. Figure 4 shows a slice image. The clear spots correspond to the denser material (fiber), while the dark gray are the pores (fluid). Then, the 2D images were submitted to the process thresholding (transformation of the gray scale image to binary scale) using different methods that imageJ offers. The methods used were IsoData, IJ-IsoData, Li, MaxEntropy, Mean, Moments, Default, Huang, Otsu, and Shanbhag. After selecting the threshold method (binarization), which permits the conversion to white and black pixels, porosity can be computed. Black pixels are associated with the skeleton and white pixels to the fluid. Porosity is given by the ratio of the number of white pixels and total of number of white and black pixels. Figure 4 and 5 show the result obtained when using the Otsu's thresholding method.

Figure 4: Original image.

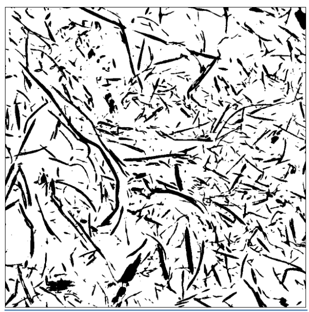

Figure 5: Processed image.

Table 3shows the results of the porosity values for the different threshold methods. It can be observed that different threshold methods yield different values for porosity. The values of the porosity present a range of variation between 0.76 and 0.96, which means a dispersion of 0.2. Huang, Li, and Mean methods present lower values of porosity, while Moments and Shanbhag methods present higher values of porosity.

Table 1: Results of porosity using different thresholding methods.

Method	Default	Huang	Isodata	IJ-Isodata	Li	Max Entropy	Mean	Moments	Otsu	Shanbhag
Porosity	0.86	0.78	0.83	0.86	0.78	0.82	0.78	0.9	0.85	0.97

To apply the histogram-based grey scale image method proposed by Taud et al., the CT image was read within MATLAB© and a histogram with 100 bins was built, as shown in Figure 3. The results of the porosity values obtained for the first slice (slice number 150) are shown in Figure 7. In the case of one slice this plot is not conclusive, as many local minima are present. Proceeding with the computation of this curve for all the 790 slices of the sample and averaging the one obtains, as presented on the plot on Figure 8, the porosity can be estimated to be 0.86.

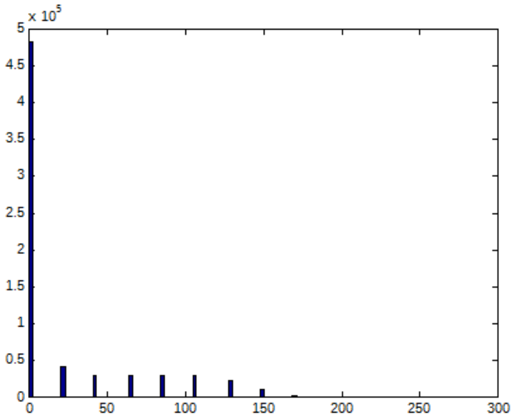

Figure 6: Tomographic 3D image reconstruction of a porous sample under study.

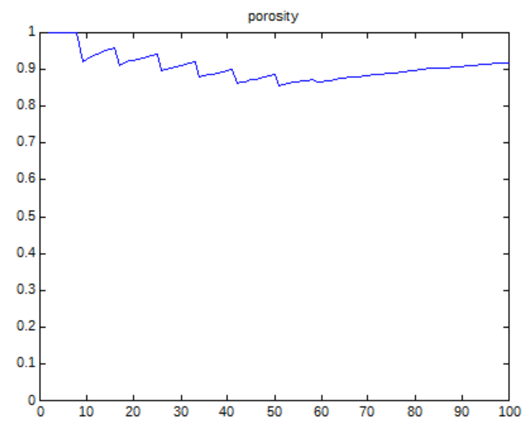

Figure 7: Original image.

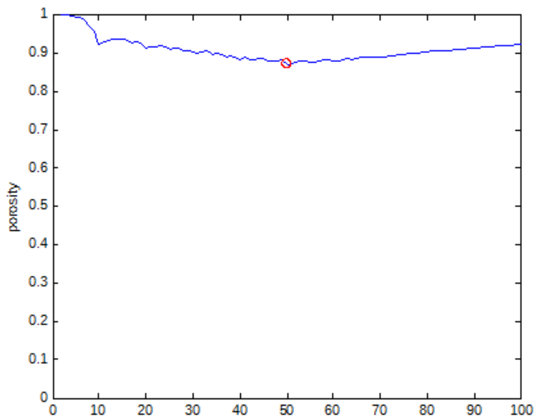

Figure 8: Processed image.

4. NUMERICAL METHODS AND THE FINITE ELEMENT METHOD

The governing idea of numerical simulation is to take benefit of the morphology of the specimen to carry out micro-scale calculations with given conditions in order to deduce macro-scale proprieties. At this stage, our objective is to evaluate the capability of some methods in order to orient our work. The tomograph is able to produce finite element meshes of the boundary of the fibres and/or volumic meshes. The figures 9 and 10 show a specimen from its FE mesh definition obtained using Avizo software. The 3D mesh of the fibres consist in 355'978 nodes and 1'643'866 Tetrahedron elements. The computed porosity (from the finite element mesh of the sample) is 0.68. Several limitations were encountered from computer performance limitation (only a 5x5x5 mm^3 specimen was meshed instead of a 40x40x40 mm^3) to modelling considerations (poor mesh quality). That is why we turned our attention to possible calculations at the pixels size. The Lattice Boltzmann Method is a possible method because the lattice can be directly built from the pixels. Concerning the FE method, we intend to construct a quad-tree mesh of voxels constructed from the slice by slice image processing. Calculations will be carried out in in the frequency domain using fluid viscous finite element derived of Navier-Stokes equations. In this case, each FE voxel will have the same "stiffness" matrix. It should accelerate the matrices assembly process and should help to control the conditioning of the global matrix system to be solved. Ongoing development are carried out considering 2D simulations because the counterpart of the approach is the needed large size calculation.

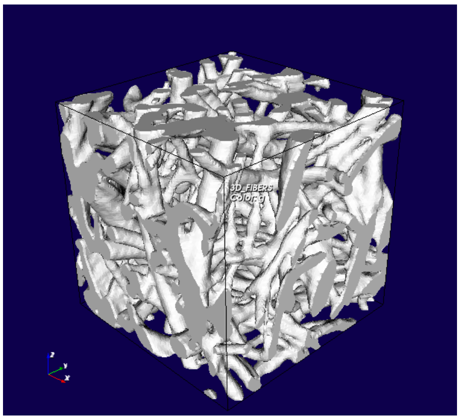

Figure 9: FE image of a 5x5x5 mm3 region of the sample.

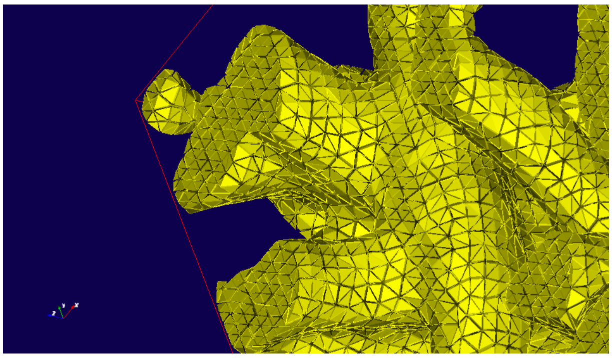

Figure 10: FE Zoom showing the tetrahedron meshing of the fibres.

5. ESTIMATING THE RESISTIVITY USING LATTICE BOLTZMANN METHOD (LBM-BGK)

As mentioned before, the LBM is attractive because the lattice can be directlty the pixels grid of the image and because the LBM is able to solve Navier-Stokes equation in the temporal domain. By this mean, and doing a stationary calculation, the static air flow resistivity can be determined. Figure 11 presents the slice that will be computed. The sample will be submitted to a flow of air from left (inlet) to the right (outlet). As a load condition, a pressure is imposed indirectly by specifying an initial imposed deformation. It is important to verify the conditions of periodicity imposed to obtain the solution of the problem (RVE - Representative Volume Element).

Figure 11: Image used for LBM calculation - Crop sample of 40x40x40 mm3.

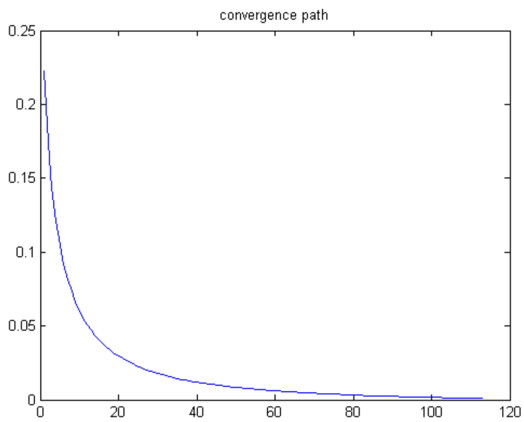

Figure 12: LBM Calculation - Iteration convergence curve.

The air flow is then calculated on the porous grid considered as obstacles to the flow. Other relevant properties of the fluid has to be settled to carry out the simulation. The main references we used are the following: Bhatnagar *et al.* (1954), Chen *et al.* (1992), Chen and Doolen (1998) Frisch *et al.* (1987) and Derksen (2007). The original software used in this work is in the public domain, authored by Sebastien Leclaire (2014) and a version of the code in Matlab is available in Iain Haslam (www.exolete.com/lbm/). In order to evaluate the results of the implemented methodology, five slices were tested of a total population of 200 slices (2D images). The velocity field results, contour of velocities in the x and y directions were analysed. The computation of the permeability is carried out through Eq. 2, as:

$$K_{Darcy} = \frac{V_m \phi}{(dP/dx)(\mu)} \tag{2}$$

with ϕ being the porosity, $V_m = \frac{\int_A u_x da}{\int_A da}$, the velocity , dP/dx, the imposed internal pressure gradient and μ the fluid dynamic viscosity.

Using a criterion based stop average speed V_m, when the range of values exceeded the relative tolerance of 0.001, the problem was considered converged. For the 5 computed slices all results were consistent. For the given example, the number of iteration at convergence is 156, the computation lasts 1 minute on a standard Laptop and a small amount of Memory is needed, only 500 Mo. Figure 12 shows the rate of convergence of the method. Typical result are presented in Figures 13, 14, 15 and 16 where the velocity field is plotted. The static viscous permeability K_{Darcy} is computed by the code and can be linked to the static air flow resistivity σ by,

$$\sigma = \frac{K_{Darcy}}{\mu} \tag{3}$$

The numerical value of the resistivity is not given because we have not not yet analysed the results in terms of physics. The method shows itself attractive. Next step will be concerned by the analyses of the physical results and by 3D simulations.

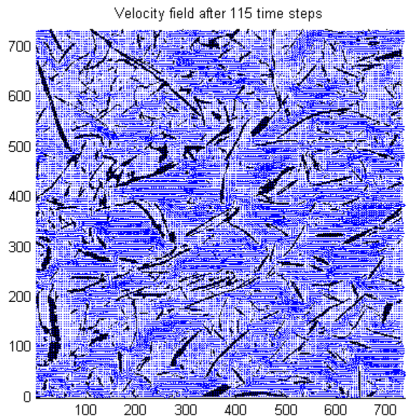

Figure 13: LBM results - Vectorial velocity field.

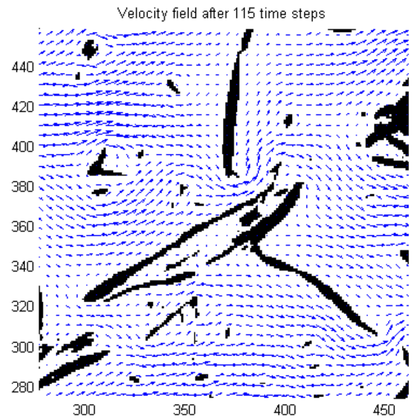

Figure 14: LBM results - Zoom showing the velocity field around the fibres.

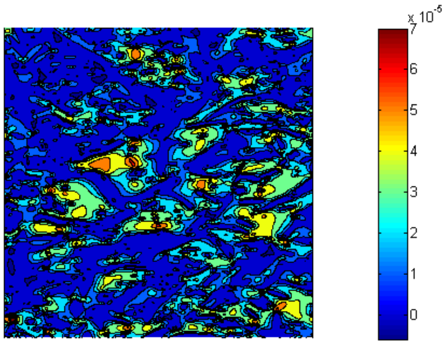

Figure 15: LBM results - Velocity field along the x-direction of the input flow.

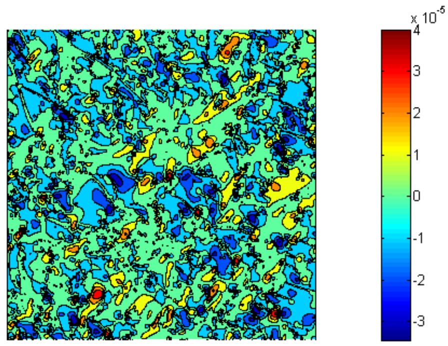

Figure 16: LBM results - Velocity field along the y-direction orthogonal to the input flow.

6. CONCLUSION

These preliminary results explore the possibility of estimating the porosity of a fibrous acoustic material using X-ray Computed Tomography. Several algorithms were compared when analysing the porosity of slices of the porous samples. Finally a mean porosity is deduced considering a large set of slices and a large set of methods. Concerning the numerical method, the Lattice-Boltzmann method shows itself very attractive from a computational point of view to compute the resistivity of the sample. The method has several prerequisites of theoretical nature related to fluid mechanics and methods for numerical approximation. Despite complex theoretical foundations, its implementation is relatively simple and the method has a great potential. It solves many classic problems of fluid mechanics with relative higher efficiency when compared to variational methods as the method of Finite Element. It is expected that the results serve as a basis for calculating the macroscopic properties of coconut fibres porous materials and can be incorporated into a larger characterization methodology. Future work will also focus on the generation of a representative volume of the material scanned with the XRCT. We intend to generate a 3D model of the actual fibrous material. This 3D model, among which the fiber properties estimated in former works, will be used in a vibroacoustic Finite Element model (FEM) to simulate its acoustic properties and compare the results with results obtained using homogenized, approximate Biot-Allard and JCA Finite Element models. These numerical model simulations aim at a deeper comprehension of the acoustic behavior of this material and at developing better homogenized models for it.

7. ACKNOWLEDGEMENTS

The authors would like to thank the Capes-Cofecub, project number 773/13, for its financial support.

8. REFERENCES

AFPC-AFREM, 1997. "Détermination de la masse volumique apparente et de la porosité accessible à l'eau. méthodes recommandées pour la mesure des grandeurs associées à la durabilité". In *Compte-rendu des Journées Techniques, Toulouse, 11-12 Décembre 1997*. pp. 121–124.

Allard, J.F. and Attala, N., 2009. *Propagation of Sound in Porous Media: Modeling Sound Absorbing Materials*. 2nd Edition, Wiley.

Bhatnagar, P., Gross, E.P. and Krook, M.K., 1954. "A model for collision processes in gases i. small amplitude processes in charged and neural one-component system". *Physics Review*, Vol. 94, pp. 511–525.

Chen, S. and Doolen, G.D., 1998. "Lattice-boltzmann method for fluid flows". *Annual Review Fluid Mechanics*, Vol. 30, pp. 329–364.

Chen, S., Wang, Z., Shan, X.W. and Doolen, G.D., 1992. "Lattice-boltzmann computational fluid dynamics in three dimensions". *Journal of Statistical Physics*, Vol. 68, pp. 379–400.

Coser, L.F., Oliveira, A., Huallpa, B.N., Arruda, J.R.F. and Siviero, D.A., 2015. "Numerical and experimental studies of a poroelastic material using the jca model." In *SAE international, 2015-36-0106*.

Coser, L.F., Siviero, D.A., Huallpa, B.N., Arruda, J.F.R., Pegoretti, T.S. and Lamary, P., 2014. "On the experimental inverse characterization of acoustic poroelastic materials using an impedance tube." In *Proc. of the 33rd Int. Conf. on Noise and Vibration Engineering (ISMA2014)*. Leuven, Belgium, September 15-17, pp. 2029–2042.

Derksen, J., 2007. "The lattice-boltzmann method for multiphase fluid flow simulations and euler-lagrange large-eddy simulations". In Springer, ed., *Multiphase Reacting Flows: Modeling and Simulation*, Springer, 2007, New York.

Frisch, U., d'Humieres, D., Hasslacher, Lallemand, P., Pomeau, Y. and Rivet, J.P., 1987. "Lattice gas hydrodynamics in two and three dimensions". *Complex Systems*, Vol. 1, pp. 649–707.

Glasbey, C.A., 1993. "An analysis of histogram-based thresholding algorithms". *CVGIP: Graphical Models and Image Processing*, Vol. 55, pp. 532–537.

Huang, L.K. and Wang, M.J.J., 1995. "Image thresholding by minimizing the measures of fuzzinesss". *Pattern Recognition*, Vol. vol 23 No. 1, pp. 41 – 51.

Keller, A., 1998. "High resolution, non-destructive measurement and characterization of fracture apertures". *nt. Journal Rock Mech. Min. Sci.*, Vol. 35(8), pp. 1037–1050.

Li, C.H. and Lee, C.K., 1993. "Minimum cross entropy thresholding". *Pattern Recognition*, Vol. 26, No 4, pp. 617–625.

Otsu, N., 1979. "Image thresholding by minimizing the measures of fuzzinesss". *IEEE Transactions on systems, Man, and Cybernetics*, Vol. SMC-9, No. 1, January, pp. 62 – 66.

Pegoretti, T.S., Coser, L.F., Siviero, D.A., Huallpa, B.N., Arruda, J.R.F. and Lamary, P., 2014. "On the experimental inverse characterization of acoustic poroelastic materials using an impedance tube: Numerical issues". In *Proc. of PACAM XIV*. 14th Pan-American Congress of Applied Mechanics, Santiago, Chile, March 24-28, 2014, pp. 1–6.

Pennafort, L.C.G., 2014. *Aplicação da mecânica da danificação na analise do comportamento de materiais compósitos poliméricos reciclados reforçados por fibras de coco*. Ph.D. thesis, Universidade Federal de Ceará.

Ridler, T.W. and Calvard, S., 1978. "Picture thresholding using an iterative selection method". *IEEE Transactions on Systems, Man and Cybernetics*, Vol. 8, pp. 630–632.

Salissou, Y. and Panneton, R., 2007. "Pressure/mass method to measure open porosity of porous solids". *J. Appl. Phys.*, Vol. 101, 2007, 124913: 1-7.

Shanbhag, A.G., 1994, September. "Utilization of information measure as a means of image thresholding". *CVGIP: Graphical Models and Image Processing*, Vol. vol 56 No 5, pp. 414–419.

Taud, H., Martinez-Angeles, R., Parrot, J.F. and Hernandez-Escobedo, L., 2005. "Porosity estimation method by x-ray computed tomography". *J. Petroleum Sci. and Eng.*, Vol. 47, pp. 209–217.

Tsai, W.H., 1985. "Moment-preserving thresholding: a new approach". *Computer Vision, Graphics, and Image Processing*, Vol. 29, pp. 377–393.

9. AUTORS RESPONSABILITY

Contents of this manuscript are authors' responsibility.